

ORIGINAL ARTICLE

Proteomics of old world camelid (*Camelus dromedarius*): Better understanding the interplay between homeostasis and desert environment



Mohamad Warda ^{a,b,*}, Abdelbary Prince ^a, Hyoung Kyu Kim ^c, Nagwa Khafaga ^d, Tarek Scholkamy ^e, Robert J. Linhardt ^f, Han Jin ^c

^a Department of Biochemistry, Faculty of Veterinary Medicine, Cairo University, Giza, Egypt

^b Biotechnology Center for Services and Researches, Cairo University, Giza, Egypt

^c National Research Laboratory for Mitochondrial Signaling, Department of Physiology, Cardiovascular and Metabolic Disease Center, Inje University, Busan 614-735, Republic of Korea

^d Animal Health Research Institute, Dokki, Giza, Egypt

^e Field Investigation Department, Animal Reproduction Research Institute, Giza, Egypt

^f Center for Biotechnology and Interdisciplinary Studies, Rensselaer Polytechnic Institute, Troy, NY 12180, USA

ARTICLE INFO

Article history:

Received 22 January 2013

Received in revised form 4 March 2013

ABSTRACT

Life is the interplay between structural–functional integrity of biological systems and the influence of the external environment. To understand this interplay, it is useful to examine an animal model that competes with harsh environment. The dromedary camel is the best model that thrives under severe environment with considerable durability. The current proteomic study

Abbreviations: 2D, two-dimensional; MS, mass spectrometry; CHAPS, 3-(3-cholamidopropyl)-dimethylammonio propane sulfonate; pI, isoelectric point; IPG, immobilized pH gradient; DTT, dithiothreitol; SDS, sodium dodecylsulfate; PAGE, polyacrylamide gel electrophoresis; TFA, trifluoroacetic acid; MALDI, matrix assisted laser desorption ionization; CHCA, α -cyano-4-signal-to-noise; ACTH, adrenocorticotropic hormone; PMF, peptide mass finger printing; PDB, protein database; TOF, time of flight; hsp, heat shock protein; MAPK, map kinase; Dvl, dishevelled: scaffold protein involved in the regulation of the Wnt signaling pathway; DAPLE, Dvl-associating protein with a high frequency of leucine residues.

* Corresponding author. Tel.: +20 2 35682195/35720399; fax: +20 2 35725240/35710305.

E-mail address: maawarda@eun.eg (M. Warda).

Peer review under responsibility of Cairo University.



Production and hosting by Elsevier

Accepted 13 March 2013
Available online 20 March 2013

Keywords:

Camel
Proteome
Metabolism
Crystallin
Actin
Vimentin

on dromedary organs explains a number of cellular mysteries providing functional correlates to arid living. Proteome profiling of camel organs suggests a marked increased expression of various cytoskeleton proteins that promote intracellular trafficking and communication. The comparative overexpression of α -actinin of dromedary heart when compared with rat heart suggests an adaptive peculiarity to sustain hemoconcentration–hemodilution episodes associated with alternative drought-rehydration periods. Moreover, increased expression of the small heat shock protein, α B-crystallin facilitates protein folding and cellular regenerative capacity in dromedary heart. The observed unbalanced expression of different energy related dependent mitochondrial enzymes suggests the possibility of mitochondrial uncoupling in the heart in this species. The evidence of increased expression of H⁺-ATPase subunit in camel brain guarantees a rapidly usable energy supply. Interestingly, the guanidinoacetate methyltransferase in camel liver has a renovation effect on high energy phosphate with possible concomitant intercession of ion homeostasis. Surprisingly, both hump fat tissue and kidney proteomes share the altered physical distribution of proteins that favor cellular acidosis. Furthermore, the study suggests a vibrant nature for adipose tissue of camel hump by the up-regulation of vimentin in adipocytes, augmenting lipoprotein translocation, blood glucose trapping, and challenging external physical extra-stress. The results obtained provide new evidence of homeostasis in the arid habitat suitable for this mammal.

© 2013 Cairo University. Production and hosting by Elsevier B.V. All rights reserved.

Introduction

One humped camel (*Camelus dromedarius*) is a unique creature belonging to old world camelid that is adapted for desert life. These camels are found mainly in the Middle East with extension into tropical and subtropical areas. With drought becoming an increasingly common global threat, the peculiar nature of the camel to cope with hot and arid conditions makes it a strategically important animal. For 14 centuries, the dromedary has been referred to as a creature of wonder [1] having a special ability to both conserve and store water. The camel can survive long periods even after more than 40% loss of its body hydration. Moreover, camels can drink as much as 57 l of water in a short period of time; such rapid rehydration is capable of causing death to other mammals.

The camel shows a true rumination pattern of digestion, expected for a ruminating ungulates; however, based on anatomical and physiological issues, it is considered as pseudo-ruminant. The camel also has the highest blood glucose level among all ruminants with similarly high glucagon levels [2].

Dromedary red blood cells have an unusual elliptical shape, possibly to facilitate their flow in the dehydrated animal. These cells are also showing less osmotic fragility than red cells in other mammals [3]. Thus, the camel's red blood cells can withstand high osmotic variation without rupturing, even during rapid rehydration. This may result from altered membrane phospholipids distribution in its red blood cells [4]. Interestingly, as a result of having very efficient kidneys, the camel urine is as thick syrup and feces are so dry that they can fuel fires [5]

Sporadic research has led to discoveries of the uniqueness of dromedary, but our understanding of this domestic ruminant is still in its infancy. For example, camelids have an unusual immune system, where part of the antibody repertoire is devoid of light chains [6]. The role of the camel's immune system to their resistance to hot arid environments is currently unknown. The current systemic study attempts to elucidate the molecular basis for the adaptive changes required for the camel's survival in an arid environment. The peculiarity of dromedary camel among mammals turns our eyes to study

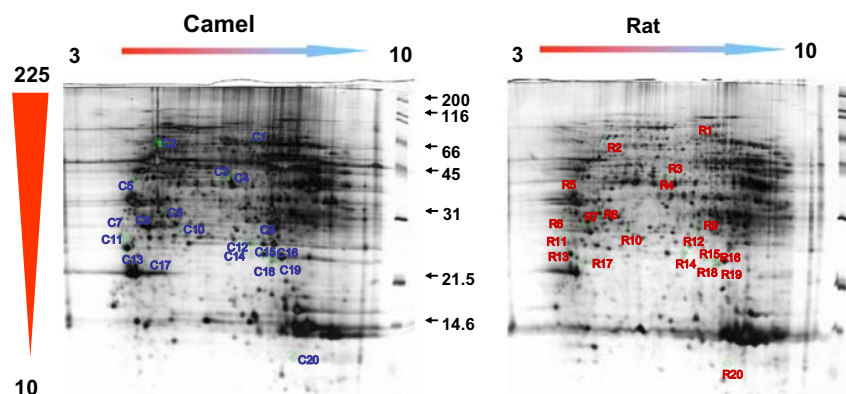


Fig. 1 Camel and rat heart proteins. In the 2D electrophoresis gel images (pH range: 3–10; with 10–225 MW range) approximately 1330 ± 95 spots were detected in each gel. The 20 significantly changed protein spots (marked spots) were selected for further MALDI-TOF MS analysis.

Table 1 Identified heart proteins in NCBI database search GI; NCBI gene bank ID, Mw; molecular weight, pi; isoelectric point, $\Delta C/R$: relative change (camel/rat%).

Camel heart							
Spot no.	Identified AA sequence (MS/MS)	MATCHED protein	NCBI acc no.	Score	Mr/pi	Seq.cov	$\Delta C/R$
C2	R.KPLVIIAEDVDGEALSTLVLNR.L R.AAVEEGIVLGGGCALLR.C	Heat shock protein 65 (<i>Mus musculus</i>)	51455	103	60903/5.48	7	49
C3	K.APIQWEER.N K.TPYTDVNIIVTIR.E R.IAEFAFEYAR.N	NAD ⁺ isocitrate dehydrogenase, alpha subunit (<i>Macaca fascicularis</i>)	1182011	183	36777/5.72	8	201
C4	MS, 11 PEPTIDE MATCHED FROM 65	3-Hydroxy-3-methylglutaryl Co-enzyme A reductase	2648815	64	47116/7.65		213
C5	K.IWHHTFYNELR.V K.SYELPDGQVITIGNER.F	Gamma non-muscle actin (<i>Oryctolagus cuniculus</i>)	1703	128	41729/5.30	7	35
C6	K.IWHHTMYNELR.V R.GYSFVTTAER.E K.SYELPDGQVITIGNER.F	Muscle actin (<i>Styela clava</i>)	10111	121	42040/5.29	9	280
C7	MS, 6 PEPTIDE MAT FROM TOTLA 65	Histone deacetylase HDAC3 (<i>Oryza sativa</i>)	50906299	49	56469/5.54		34
C8	K.AHGGYSVFAGVGER.T R.VALTGLTVAEYFR.D R.DQEGQDVLLFIDNIFR.F	ATP synthase beta subunit (<i>Oncorhynchus mykiss</i>)	76362315	215	18719/4.87	24	29
C11	R.VGWELLTIIAR.T K.GITQEQMNEFR.A R.ASFNHFDR.R R.ETADTDTAEQVIASFR.I R.ILASDKPYILAEELR.R	Actinin, alpha 2 (<i>Homo sapiens</i>)	4501893	229	103788/5.31	6	984
C12, 13	K.IEFTPEQIEEFKEAFMLFDR.T K.ITYGQCGDVL.R.A R.ALGQNPTQAEVLR.V K.NKDTGTIEDFVEGLR.V K.DTGTIEDFVEGLR.V	PREDICTED: similar to myosin light polypeptide 3	57101266	445	22355/5.02	29	286
C 15	R.RPFFPFHSPSR.L R.APSWIDTGLSEMR.L R.IPADVDPLAITSSLSDGVL	Alpha B-crystallin chain	73954784	212	20054/6.76	28	773
C 16	R.RPFFPFHSPSR.L R.APSWIDTGLSEMR.L R.IPADVDPLAITSSLSDGVL	Crystallin, alpha polypeptide 2-.Hsps	27805849	183	20024/6.76	28	321
C18	R.RPFFPFHSPSR.L R.APSWIDTGLSEMR.M	Alpha B-crystallin polypeptide 2 (<i>Rattus rattus</i>)	57580	99	19945/6.84	13	320

its proteome in comparison with rat. The choice of rat as a generally accepted central point mammalian model expands our scope of comparison beyond the limited frame of ungulates. Proteomic differences between different organs in the camel and the rat are examined by two-dimensional (2D) mass spectrometry (MS/MS)-enabled 2D electrophoresis. This study affords a better understanding of the interplay between mammalian homeostasis and a harsh environment.

Material and methods

Tissues

Healthy, clinically normal adult male one humped camels (*Camelus dromedarius*) were used in the study. Animals were kept on rest with food and water ad libitum one week before

slaughtering. Liver, heart, brain, kidney, and hump fat from camels were collected and cut into thin slices at an authorized abattoir house (Giza District, Egypt). At least five animals were sampled for each organ. Samples were snap-frozen in liquid nitrogen and stored in -70°C until processing. The collection and use of these samples was approved by the Institutional Review Board of Egyptian Animal Health Affairs. Samples of the same organs were similarly prepared from rat (*Rattus norvegicus*) maintained at the animal care unit (Medical School – Inje University, Republic of Korea).

2D-gel electrophoresis and proteomics

Protein samples from camel organs were examined in parallel with rat control organs. Proteins were extracted for 2D gel electrophoresis using a 2D Quant kit (GE Healthcare) as

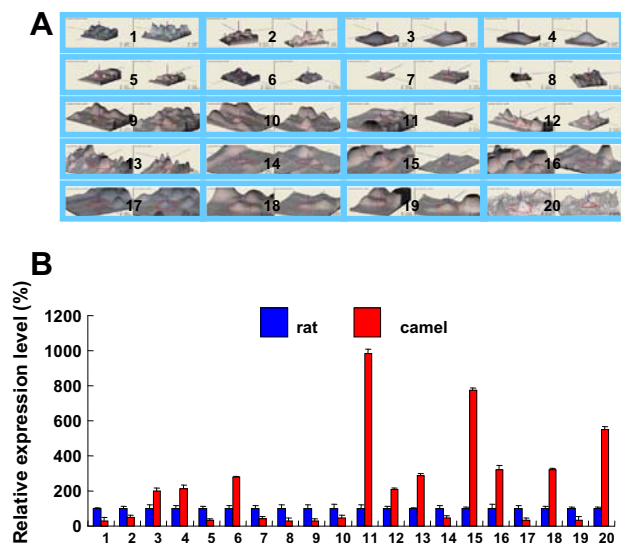


Fig. 2 Camel and rat heart proteins. (A) Enlarged three-dimensional electrophoresis spots images showing the 10 overexpressed and 10 under expressed protein spots. (B) Histograms quantify these protein spots. (The error bars represent the SEM of mean of at least three independent experiments, $p < 0.05$ vs control) (pH range: 3–10; with 10–225 MW range).

previously described [7] and described in Supplementary data sheet 1.

Image analysis

Silver-stained gels were scanned on a flatbed scanner (Umax PowerLook 1100; Fremont, CA, USA), and the resulting digitized images were analyzed using ImageMaster 2D Platinum software (GE Healthcare). At least three separate gels of the same organ from different animals were independently analyzed to increase experimental certainty. Further gel analysis was performed as previously described [8,9] and listed in Supplementary data sheet 2.

Protein mass analysis and identification

The selected stained spots were excised, destained, reduced and digested with trypsin. Peptides were analyzed with matrix assisted laser desorption ionization (MALDI) TOF/TOF mass spectrometer, 4700 Proteomics Analyzer (Applied Biosystems, Framingham, MA) for protein identification [7,8]. Resulting data were analyzed by GPS Explorer™ 3.5 (Applied Biosystems) software. The proteins were identified by using MASCOT 2.0 search algorithm (Matrix Science, London) to search rodent subset of the National Center for Biotechnology Information (NCBI) protein databases.

Results

Data handling

The logical evaluation of the camel proteome is complicated by the absence of previously published genomic and proteomic data. Since rat (*Rattus norvegicus*) is a well known mammalian

model with many Protein Data Bank (PDB) entries, the proteome of corresponding rat organs was used as the reference control. The protein levels in various camel organs were visualized on 2D electrophoresis gels. Based on an automated spot-counting algorithm (Image Master 2D Platinum), means of 1325 ± 95 protein spots were detected in the gel of the heart, liver, adipose tissue, kidney, and brain. All spots were distributed in the region of pI 4–9 and had relative molecular weights (MW) between 15 and 200 KDa. The protein spots in both camel and control gels were then excised from the gel and incubated with trypsin to digest the proteins in the gel, which were then analyzed by MALDI-time of flight (TOF) MS/MS.

Camel heart proteome

The camel heart proteome showed a well matched proteomic image to that of the rat heart control (Fig. 1 and Table 1). It is clear that actinin and alpha B-crystallin were markedly overexpressed in camel compared to that of the control (Fig. 2). In the 2D electrophoresis-MS/MS data, alpha B-crystallin in camel heart showed peptides (Fig. 3A) that covered both conserved domains of bovine alpha B-crystallin [*Bos taurus*] as well as the intervening peptides (57–69 amino acid residues). These results demonstrate a strong identity between camel and bovine alpha B-crystallin with possible two sites for phosphorylation. Despite a twofold increase in the expression of NAD⁺-dependent isocitrate dehydrogenase in camel heart when compared to the rat heart, there was a parallel down regulation of ATP synthase expression. Moreover, all the overexpressed proteins had acidic pIs.

Physical distribution of the camel proteome

Camel heart proteomic data closely matched its counterpart rat proteome. To amplify the differences in proteomic data from the remaining organs, each gel was divided into four quarters and proteins separated based on MW and pI. The relative abundance of proteins in each group was estimated from the total number spots, and the percent area in each quarter gel occupied by proteins as revealed by gel imaging. These data were then compared to the corresponding quarters in rat control for liver adipose tissue and kidney (Fig. 4A–C). Interesting, both adipose tissue and kidney proteomes shared a higher density of acidic proteins (pI < 7). While these acidic proteins are concentrated in the low molecular weight range in hump adipose tissue, in the kidney proteome, these acidic proteins displayed a wide range of molecular weights.

Camel liver proteome

The camel liver proteome was dissimilar to the rat liver control. An area of well defined dimensions (pH and MW) was selected in that showed marked similarity by visual and digital inspection (Fig. 5A). The protein spots within these clearly defined boundaries were then analyzed by MALDI-TOF MS or MS/MS. The proteins identified in camel proteome with no corresponding counterpart in the rat control are representative of overexpressed proteins. To determine the amino acid sequence of proteins of camel proteome that does not match with the known proteome MS database, the MS/MS was then performed.

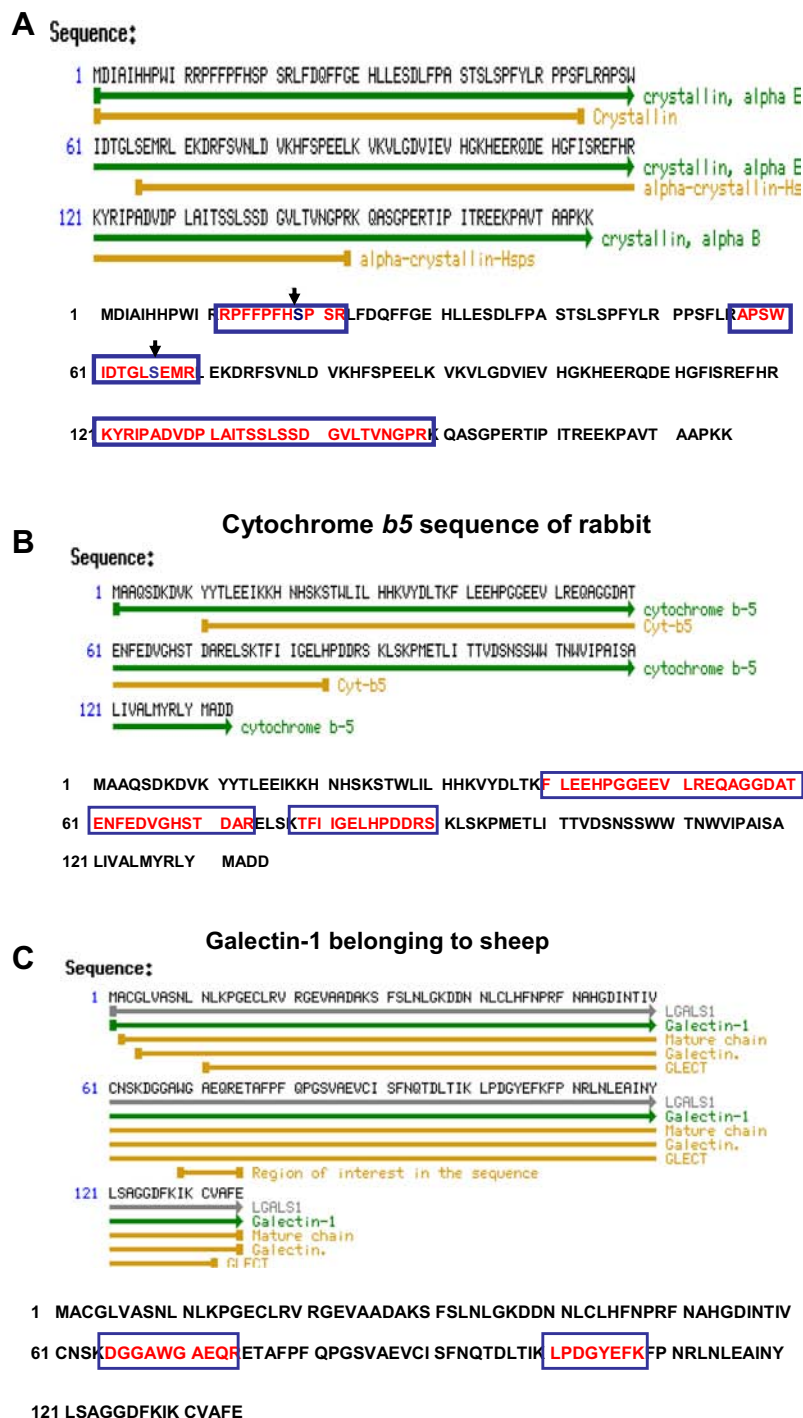


Fig. 3 Comparative analysis of sequence data obtained from the camel proteome. (A) α -B-crystallin belonged to bovine [*Bos Taurus*; gi:117384; top] showing the MS/MS-derived matched sequences in camel α -B-crystallin (red-marked with blue boxes sequences; bottom). The reported sequences in camel cover both conserved domains of bovine crystallin, α -B with marked identity to bovine one and possible two serine phosphorylation sites (indicated by arrows). (B) Cytochrome b5 sequence of rabbit [*Oryctolagus cuniculus*] (top) and the shared amino acids sequence residues with that indicated by MS/MS data for camel adipose tissue (bottom). The shared sequences of camel with that of rabbit cytochrome b5 (gi:164785) are red-marked in blue boxes. The matched sequences carry different motives that responsible for the final enzyme activity. (C) Galectin-1 belonging to sheep [*Ovis aries*]. The sequence shown in red with blue framed box is the MS/MS-reported matched sequences in camel galectin-1. The specific region of interest in reported sequence of sheep (69–75 amino acid residues; WGAEQRE gi:3122339) is included with the matched camel sequence. (D) Bovine [*Bos Taurus*] phosphatidylethanolamine binding protein (gi:1352725) sequence. The MS/MS-matched amino acid residues in camel brain proteome (shown in red in blue framed box) are proved to have interspecies similarities in Beta-strand region (Res. # 62–70); hydrogen bonded turns (Res. # 71–72 and Res. # 94–95); helical region (97–99), and second Beta-strand region (Res. # 100–104).

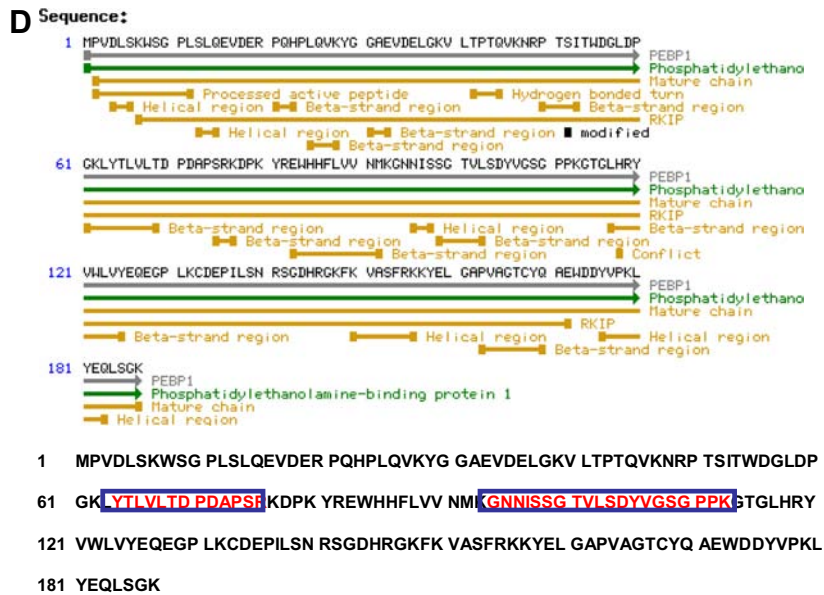


Fig. 3 (continued)

The results of proteins were identified by MS, MS/MS for liver of camel and rat, respectively (Tables 2 and 3). The amino acid sequence from MS/MS of the guanidinoacetate methyltransferase (Fig. 6) matched this same protein in the corresponding NCBI peptide database. Among the determined set of liver proteins, a total 13 proteins were identified by MS to be over 70 (Mowse score) and/or over 34 in MS/MS peptide sequencing. The liver proteome showed differential expression of metabolic enzymes and cytoskeleton proteins. In contrast to the large number of metabolic enzymes identified in rat liver within the circled area, few of these were observed in the camel proteome (Fig. 5A). The MS/MS data show the similarity of camel metabolic enzymes to those of other species.

Camel hump fat proteome

The proteome of hump adipose tissue was analyzed in comparison with adipose tissue of rat similar to that of liver (Fig 5B; Tables 4 and 5). Hump fat adipose tissue displayed many more protein spots than that of rat adipose tissue. Unlike the rat control, the proteome of camel adipose tissue contains cytoskeleton proteins together with heat shock proteins, including hsp 27, hsp 70, and vimentin (see insert circled area in Fig. 5B).

These data clearly confirm the presence of actin and tubulin cytoskeletal proteins and high abundance of vimentin, suggesting the overexpression of cytoskeleton proteins in fat cells.

Camel hump adipose tissues also actively perform glycolysis involving the Krebs cycle and hexose monophosphate pathways, as evidenced by the expression of glyceraldehydes-3-phosphate dehydrogenase, isocitrate dehydrogenase, and aldolase. The metabolic enzymes in camel adipose tissue share common domains with other species. The conserved domain of cytochrome b5 in rabbit (gi:164785) shares the same common sequence (40–89 amino acids residues) observed in camel adipose tissue as indicated by MS/MS (Fig. 3B). This finding supports the extensive homology of the conserved domain of this ortholog gene. Moreover, the present investigation suggests

the presence of galectin-1 in camel adipose tissue (Fig. 3C). The amino acid residues (residues 69–75) in the reported sequence of galectin-1 in sheep (*Ovis aries*) [gi:3122339] were among those matched by MS/MS to camel.

Camel brain proteome

A number of proteins are uniquely expressed in camel brain with no corresponding protein spots in the equivalent areas of the control. These proteins (Fig. 5C and Table 6) are either uniquely expressed or highly expressed in the brain of camel. The camel brain uniquely expresses or overexpresses chaperonin 10, chaperonin-like beta-synuclein, phosphatidylethanolamine binding protein showing marked homology to bovine brains and cytoskeleton tubulin 5-beta (Fig. 3D).

Camel kidney proteome

Camel kidney revealed only one unique, identifiable spot belonging to calbindin family of proteins (Fig. 5D and Table 7). Many protein spots failed to match the NCBI peptide MS or MS/MS database.

Discussion

The one humped camel has a unique tolerance for extremely hot and arid conditions. The observed climate change with projected environmental increase in global warming and desertation makes the dromedary camel an economically and logistically strategic animal. The absence of genomic data and a defined proteome makes understanding this important species quite challenging. Proteomic data, even in the absence of a defined genome, should lead to improved understanding of the phenotypic acclimatization of this unique mammal. The current study describes a novel approach to understand the interplay between proteome – homeostasis in the dromedary camel.

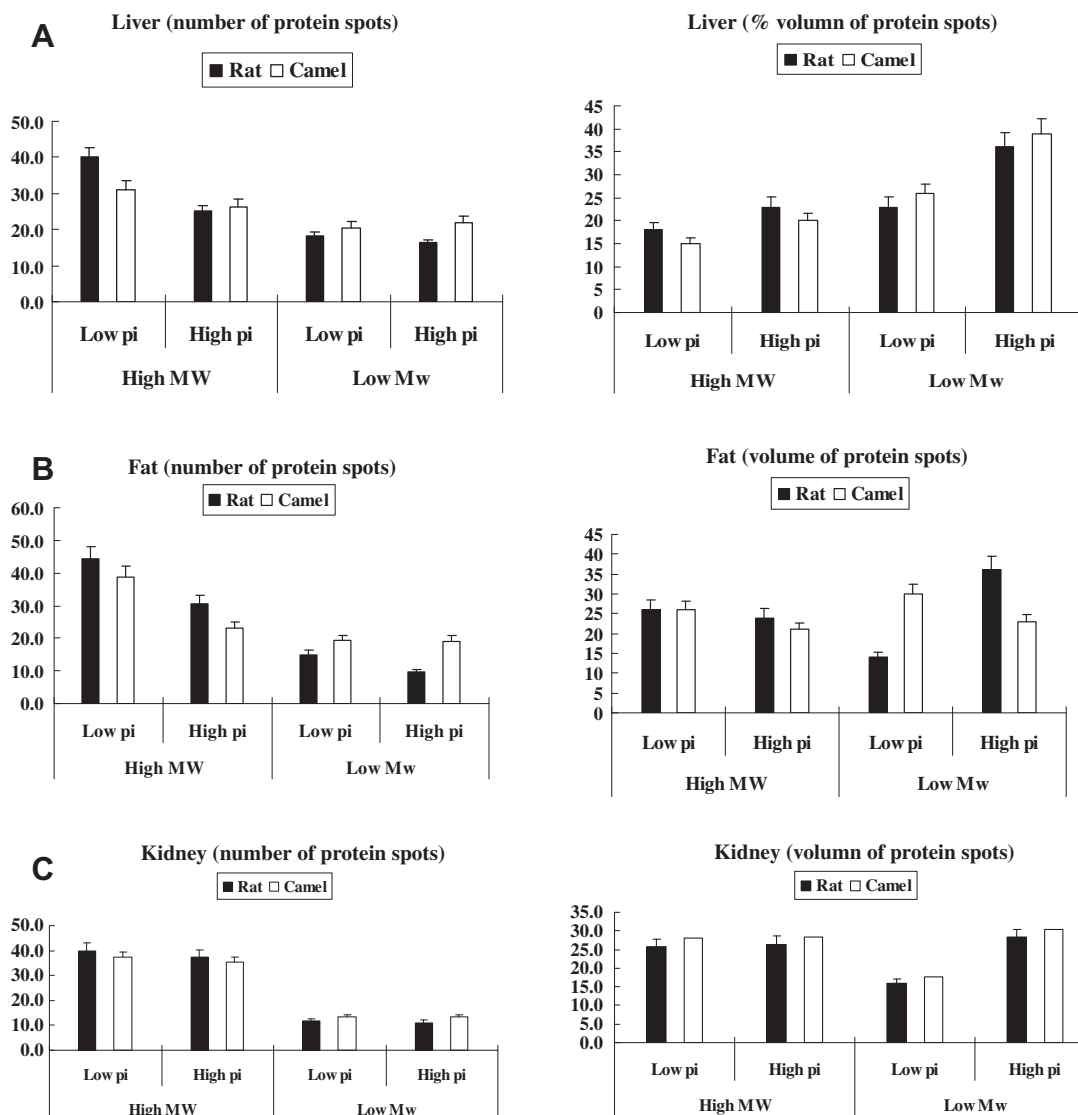


Fig. 4 The relative abundance of proteins (spot numbers and total area) in each quarter of gel that represents the proteomic images. Camel liver (4-A); hump fat (4-B); and kidney (4-C) were estimated from both total number of spots and % volume of occupied proteins (as revealed by the 3D imaging of the gels) in each quarter. The migrated proteins were, therefore, parted according to their MW and pI. The data were then compared with corresponding quarters in rat control. Both adipose tissue and kidney proteomes shared higher clusters of acid tolerable proteins ($p < 7$). (Error bars are SEM, $p < 0.05$; $n = 3$ at least).

Camel heart proteome

Energy balance and structural integrity are indispensable elements for the optimal performance of camel heart in an arid environment. Both isocitrate dehydrogenase and ATP synthase considerably impact mitochondrial energizing of the camel heart. The relative increase in isocitrate dehydrogenase parallels a decrease in ATP synthase and represents evidence for proton leakage in camel cardiac muscle. The wide range of body temperature fluctuation accompanied by variable respiratory frequency and different level of exhaled water in desert camel [10] require a greater flexibility of camel mitochondria to move between respiratory states. Further investigation is required on camel mitochondria decoupling proteins to confirm this hypothesis.

Cardiac myocytes contain intracellular cytoskeleton scaffolds that provide for structural support, compartmentaliza-

tion of intracellular components, protein synthesis, intracellular trafficking, organelle transport within the cell, and second messenger signaling pathway modulation [11,12]. The observed overexpression of cytoskeleton proteins in camel heart greatly reduces cellular stress by offering rapid and durable tool for direct cellular communication [13].

Surprisingly, a marked up-regulation of α -actinin2 expression was observed in camel heart compared to that of the control. Alpha-actinin2 is a cytoskeleton protein belonging to the spectrin gene superfamily. This family has a wide range of cytoskeletal proteins, including the α - and β -spectrins and dystrophins. Alpha-actinin2 is an actin-binding protein with various activities in different cell types. Recent evidence also shows the involvement of α -actinin2 in molecular coupling of a Ca^{2+} -activated K^+ channel to L-Type Ca^{2+} channels giving better ion channels modulation [14]. This may result in an improved tolerance for abrupt ionic imbalance

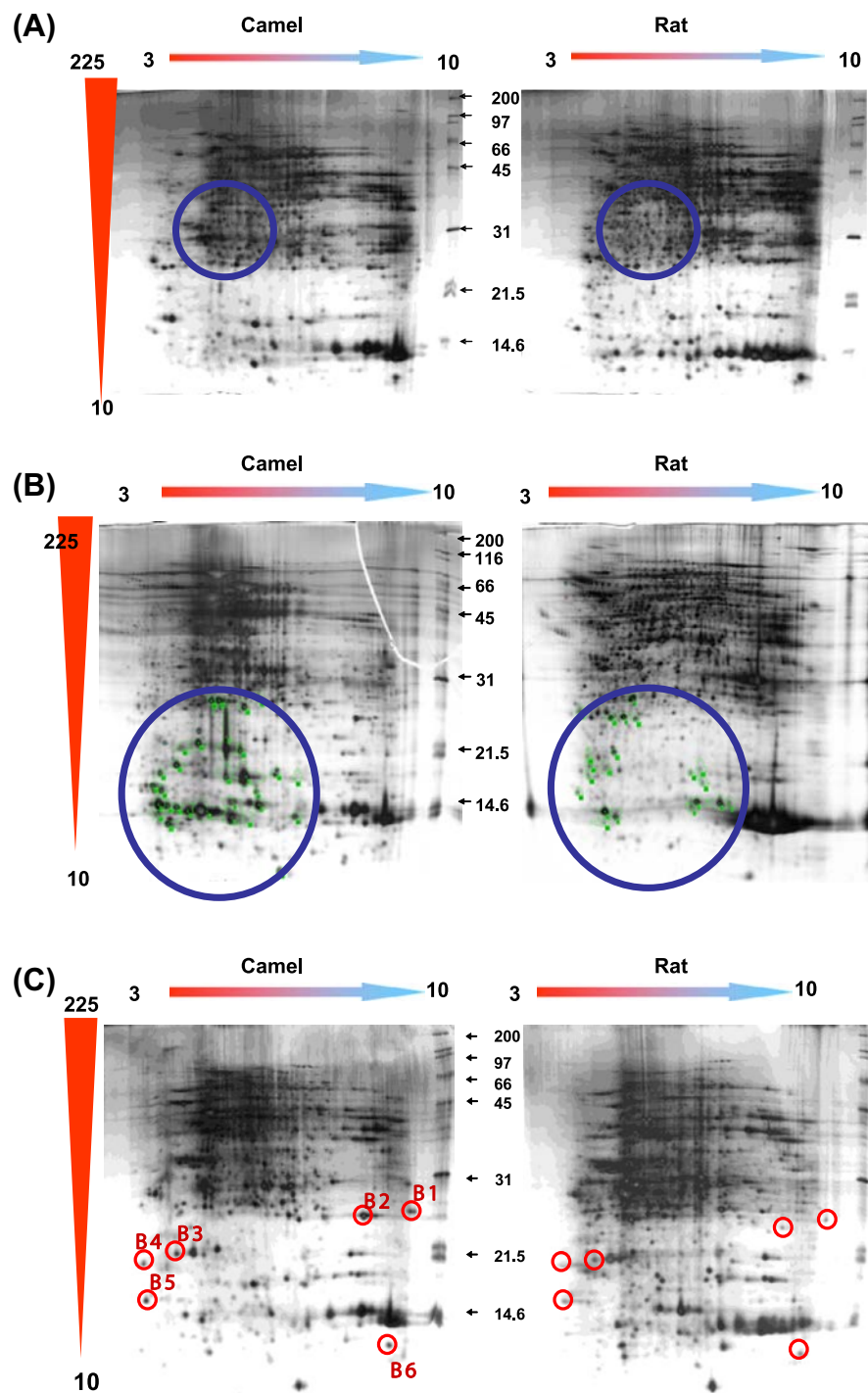


Fig. 5 2D electrophoresis gel images. (A) Camel and rat liver proteomes. Approximately 1314 ± 22 spots were detected within the blue circled area in each gel. The 27 protein spots that showed different expression in camel and rat liver were selected for further MALDI-TOF MS analysis. (B) Adipose tissues of camel hump and rat fat. Approximately 804 ± 32 spots were detected within the blue circle area in each gel. The 26 significantly changed protein spots (marked in green) were selected for further MALDI-TOF MS analysis. (pH range: 3–10; with 10–225 MW range). (C) Brain of camel and rat. Approximately 1476 ± 26.5 spots were detected in each gel. The identified protein spots that showed marked expression in camel brain (red circles) were selected for further MALDI-TOF MS analysis. (D) Kidney of camel and rat, respectively. Approximately 1641.2 ± 12.5 spots were detected in each gel. The identified protein spots that showed marked expression in camel (red circles) over that of control rat (dashed red circles) were selected for further MALDI-TOF MS analysis. (pH range: 3–10; with 10–225 MW range).

with enhanced extra-osmoregulatory capacitance of camel cardiomyocytes.

A sevenfold increase in the expression of alpha B-crystallin fits well with the protection of surrounding structural integrity

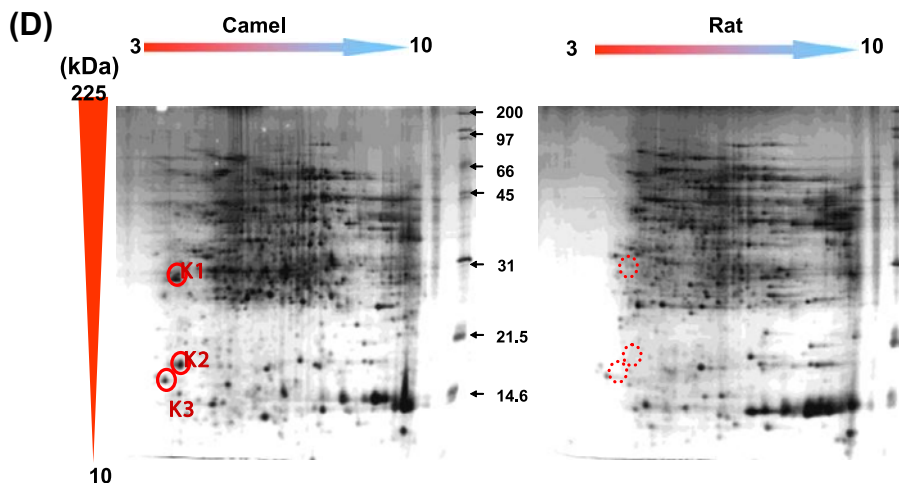


Fig. 5 (continued)

Table 2 Identified camel liver proteins in NCBI database search GI; NCBI gene bank ID, Mw; molecular weight, pI; isoelectric point.

Camel liver						
Spot no.	Identified AA sequence (MS/MS)	MATCHED protein	NCBI acc no.	Score	Mr/pI	Seq.cov
C1	R.AVFPSIVGRPR.H K.YPIEHGIVTNWEDMEK.I K.IWHHTFYNELR.V R.VAPEEHPVLLTEAPLNPK.T R.GYSFTTTAER.E K.SYELPDGQVITIGNER.F K.DLYANTVLSGGTTMYPGIADR.M	Hypothetical protein XP_533132 [<i>Canis familiaris</i>] (Actin like protein)	73964667	114	42053/5.24	27
C2	K.ELFPIAAQVDK.E R.ASSTANLIFEDCR.I K.IAMQTLDMGR.I R.ITEIYEGTSEIQR.L R.LVIAGHLLR.S	Acyl-CoA dehydrogenase (EC 1.3.99.3) precursor, short-chain-specific	111334	74	44654/8.42	13
C4	K.LAEQAERYDEMVESMK.K K.KVAGMDVELTVEER.N K.KVAGMDVELTVEER.N R.NLLSVAYK.N R.YLAEFATGNDR.K R.YLAEFATGNDRK.E K.AASDIAMTELPPTHPIR.L K.AASDIAMTELPPTHPIR.L	PREDICTED: similar to 14-3-3 protein epsilon (14-3-3E) (Mitochondrial import stimulation factor L subunit) (MSF L) isoform 1 [<i>Canis familiaris</i>]	73960520	103	26785/4.73	28
C6,7	K.GAGTDEGCLIEILASR.T R.ISQTYQQYGR.S R.SLEDDIRSDTSFMFQR.V R.SDTSFMFQR.V R.VLVLSAGGR.D K.SMKGLGTDNTLIR.V R.AEIDMLDIR.A R.AEIDMLDIR.A Oxidation (M)	PREDICTED:annexin IV isoform 5 [Pan troglodytes]	114577902	79	36258/5.84	23
C8	R.LHDVDFYK.A K.HLQKDFEQVK.E K.SLDTLQNVSVRLEGLER.D R.ELEAEHQALQR.D R.DLTKQVTVHTR.T R.KAELDELEK.V K.GEYEELHAHTK.E R.SSPTPAEVLTEAK.V	PREDICTED: similar to DVL-binding protein DAPLE [<i>Canis familiaris</i>]	73964395	71	266905/5.87	5

(continued on next page)

Table 2 (Continued)

Camel liver						
Spot no.	Identified AA sequence (MS/MS)	MATCHED protein	NCBI acc no.	Score	Mr/pI	Seq. cov
C15,17	K.ASDLPAIGGQPGPPAR.K K.MASSTSEK.L K.SDEPELLAR.L					
	M.PGGLLLGDEAPNFEANTTVGR.I R.DFTPVCTTELGR.A K.LAPEFAKR.N K.LPFIHDDKNR.D K.LSILYPATTGR.N R.NFDEILR.V	Hypothetical protein [Macaca fascicularis]	84579335	92	25109/5.74	31
	Proteins matching the same set of peptides	Antioxidant protein 2 (non-selenium glutathione peroxidase, acidic calcium-independent phospholipase A2) [<i>Bos taurus</i>]	27807167	82	25108/5.74	
C14,16,18	R.SFASSAAFEYIITAK.K R.NSNVGLIQLNRPK.A K.AQFGQPEILIGTIPGAGGTQR.L K.SLAMEMVLTGDR.I K.LFYSTFATEDRK.E K.EGMAAFVEK.R Oxidation (M)	Enoyl Coenzyme A hydratase, short-chain, 1, mitochondrial [<i>Bos taurus</i>]	70778822	80	31565/ 8.82	28
	Proteins matching the same set of peptides	Enoyl Coenzyme A hydratase, short-chain, 1, mitochondrial [<i>Rattus norvegicus</i>]	17530977	106	31895/6.41	
		Chain A, structure of enoyl-CoA hydratase complexed with the substrate Dac-CoA	20149805	106	28312/6.41	
		Chain A, crystal structure analysis of rat enoyl-CoA hydratase in complex with hexadienoyl-CoA enoyl-CoA hydratase [<i>Sus scrofa</i>]	24159081	106	28498/6.41	
C20	R.VLEVGFGMAIAATK.V oxidation (M)	Guanidinoacetate N-methyltransferase [<i>Bos taurus</i>]	84370113	44	26821/5.70	5
C27	R.AVAIDLPLGR.S R.AVAIDLPLGR.S R.GYVPVAPICTDK.I	Abhydrolase domain containing 14b [<i>Rattus norvegicus</i>]	56090461	72	22718/5.65	10

with improved regeneration. The small heat shock protein alpha B-crystallin is a molecular chaperon, which stabilizes proteins that are partially or totally undergo unfolding as a result of inflammatory stress [15]. Alpha B-crystallin, belonging to the family of ATP-independent chaperones, utilizes minimum energy to prevent misfolded target proteins from aggregating and precipitating. Cardiac crystallin is recently proved to contribute in a localized structural or protective role [16]. Furthermore, MAPK kinase MKK6-dependent phosphorylation of alpha B-crystallin shows cytoprotective effects on cardiac myocytes when they are exposed to cellular stress [17]. The overexpression of alpha B-crystallin in camel heart supports this mechanism and suggests an extra protective role against dehydrating and sudden rehydration stress in arid environments. A high level of identity was observed between bovine in both conservative domains of bovine alpha B-crystallin [*Bos taurus*] and the intervening peptides (57–69 aa). These results afford two possible phosphorylation sites in the three major serine residues (Ser19, Ser45, and Ser59) previously shown to be available for post-translational modification [18,19]. Phosphorylation enhances the chaperone activity of alpha B-

crystallin, protecting against two types of protein misfolding, amorphous aggregation, and amyloid fibril assembly in the heart [20].

Interestingly, the camel heart proteome shows a relatively similar pattern of distribution of rat heart regarding the localization based on pI scaling and molecular weight distribution.

Proteome interprets the organ uniqueness in liver morphology

Liver is a metabolically active organ contributing in many homeostatic mechanisms. The maintenance of liver activity necessitates the presence of active metabolic and energy saving enzymes, available building blocks, and the safeguarding of the newly formed biomolecules. The hepatic proteome of camel metabolic enzymes indicates a wide range of similarity with other mammals. Energy shuttling enzymes, such as ATP synthase (β -subunit), are similar in the hepatic proteome of camel and other known species. Moreover, energy related and fatty acid regulatory enzymes show a high level of identity to other species. These include citric acid cycle enzymes, NAD-dependent isocitrate dehydrogenase, members of β -oxidation of

Table 3 Identified rat liver proteins in NCBI database search GI; NCBI gene bank ID, Mw; molecular weight, pI; isoelectric point.

Spot no.	Identified AA sequence (MS/MS)	MATCHED protein	NCBI acc no.	Score	Mw/pI	seq.cov
<i>Rat liver</i>						
<i>Metabolic enzymes and enzyme like proteins</i>						
R1,R2	R.RFSSEHDIFR.E R.IFSSEHDIFR.E K.FFQEEVIPYHEEWEK.A K.CIGAIAMTEPGAGSDLQGV.R.T K.AQDTAELFFEDV.R.L R.LPASALLGEEKNGFYLLMQELPQER.L K.GFYLLMQELPQER.L R.LLIADLAISACEFMFEETR.N	Acetyl-coenzyme A dehydrogenase, long-chain [<i>Rattus norvegicus</i>]	6978431	86	48242/7.63	23
R4	K.VADIGLAAWGR.K R.KALDIAENEMPGLMR.M K.ALDIAENEMPGLMR.M R.WSSCNIFSTQDHAAAIAK.A K.GETDEEYLWCIEQTLHFK.D K.HPQLLSGIR.G K.SKFDNLYGCR.E K.FDNLYGCR.E K.EGNIFVITTTGCVDIILGR.H R.IILAEGR.L	Chain A, rat liver S-adenosylhomocystein hydrolase	4139571	123	47889/6.08	25
R6	R.DHGDIAFVDVDPNDSPFQIVK.N K.ANEQLAAVVAETQK.N K.DIVYIGLR.D R.DVDPGEHYIIK.T K.VMEETFSYLLGR.K K.VMEETFSYLLGR.K Oxidation (M) R.EGLYITEEYK.T K.TGLLSGLDIMEVNP TLGKTPEEVTR.T R.EGNHKPETDYLKPPK.-	Chain A, crystal structure Of the H141c arginase variant complexed with products ornithine and urea	13786702	125	35096/6.72	35
R7,8	R.HIDGAYVYR.N K.LWSTDHDPEMVRPALER.T K.SLGVSNFNR.R K.SLGVSNFNR.Q K.YKPVTNQVECHPYFTQTK.L R.NPLWVNVSSPPLLKDELLTSLGK.K K.TQAQIVLR.F R.FVEMLMWSDHPPEYPFHDEY.-	Aldo-keto reductase family 1, member D1 [<i>Rattus norvegicus</i>]	20302063	114	37639/6.18	31

(continued on next page)

Table 3 (Continued)

Spot no.	Identified AA sequence (MS/MS)	MATCHED protein	NCBI acc no.	Score	Mr/pI	seq.cov
R9, 11	K.CPGVPSGLETLEETPAPR.L	Aryl sulfotransferase [<i>Rattus norvegicus</i>]	55765	134	33422/6.41	38
	K.THLPLSLLPQSLLDQK.V					
	K.VKVIYIAR.N					
	K.EWWELR.H					
	R.HTHPVLYLFYEDIKENPK.R					
	K.KILEFLGR.S					
	R.SLPEETVDSIVHHTSFK.K					
	R.SLPEETVDSIVHHTSFKK.M					
	K.NTFTVAQNERFDAHYAK.T					
	K.IVGSNASQLAHFDPR.V					
	R.VTMWVFEEDIGGR.K Oxidation (M)					
	R.KLLEIINTQHENVK.Y					
	K.LTEIINTQHENVK.Y					
K.FCETITIGCKDPAQQQLL.K.E						
K.ELMQTPNFR.I						
K.ELMQTPNFR.I Oxidation (M)						
R.ITVVQVEVDITVEICGALK.N						
K.NIVAVGAGFCDFGLGFGDNTK.A						
R.ELHSILQHK.G						
R10	R.LGGEV'SCLVAGTK.C	Electron transferring flavoprotein, alpha polypeptide [<i>Mus musculus</i>]	31981826	114	35271/8.42	33
	K.VLVAQHDAYK.G					
	K.QFSYTHICAGASAFGK.N					
	K.LNVAPVSDIIEIK.S					
	R.TIYAGNALCTV.K.C					
	K.LLYDLADQLHAAV GASR.A					
	R.AAVDAGFVPNDMQVGTGK.I					
	K.VVPEMTEILK.K					
	K.VVPEMTEILK.K Oxidation (M)					
	K.MKDLHLGEQDLQPETRE					
	K.MKDLHLGEQDLQPETRE Oxidation (M)					
	K.AGTTWTQEIYDMIQNDGDVQK.C					
	R.NAKDCLVSYYYFSR.M					
K.DCLVSYYYFSR.M						
K.VLWGSWYDHYK.G						
K.GWWDVKDQHR.I						
K.FLEKDISEEVLNK.I						
R.KGMPGDWK.N						
K.NYFTVAQSEDFEDDYR.R						
R.KMAGSNITFR.T						
R13,15	13929030	Sulfotransferase family 1A, member 2 [<i>Rattus norvegicus</i>]	13929030	148	35855/6.09	39
	57527919					

R14,16	R.KMAGSNITFR.T Oxidation (M)	92087001	116	36659/6.16	35	Malate dehydrogenase, cytoplasmic (cytosolic malate dehydrogenase)
	K.MAGSNITFR.T					
	K.MAGSNITFR.T Oxidation (M)					
	K.DLDVAVLVGSMPR.R					
	K.VIVVGNPANTNCLTASK.S					
	K.SAPSIKKNFSCSLTR.L					
	K.NVIWGNHSSTQYDPVNHAK.V					
	K.EVGVEALKDDSWLK.G					
	K.GEFTTVQQR.G					
	K.FVEGLPINDFSR.E					
	K.ELTEEKETAFFLSSA.-					
	R.LFEENDINLTHIESRPSR.L					
	K.NTVPWFPR.T					
K.QFADIAYNYR.H						
R.VEYTEEEKQTWGTVFR.T						
R.LRPVAGLLSSR.D						
R.DFLGGLAFR.V						
R.VFHCTQYIR.H						
R.TFAATIPRPFVSR.Y						
R.SGVLPLWRPDSK.T						
K.TQVTQYVQDNGAVIPVR.V						
R.VHTIVISVQHNEIDITLEAMR.E						
R.FVIGGPQGDAGVTGR.K						
K.NFDLRPGVIVR.D						
K.TACYGHFGR.S						
R.AAVPSGASTGIYEALELR.D						
K.LAMQEFMILPVGASSFR.E						
R.JGAEVYHNLK.N						
K.AGYTDQVIGMDVAASEFYR.S						
R.YITPDQLADLYK.S						
K.VNQIGSVTESLQACK.L						
R.SGETEDTFIADLVVGLCTGQIK.T						
R.SFRNPLAK.-						
K.NSSVGLIQLNRPK.A						
K.AFAAGADIKEMQNR.T						
K.AFAAGADIKEMQNR.T Oxidation (M)						
R19		4930076	100	49694/5.67	21	Chain A, structure of phosphorylated phenylalanine hydroxylase
R20		77157805	85	44125/5.70	21	Methionine adenosyltransferase I, alpha [<i>Rattus norvegicus</i>]
R21,22		70794816	111	47453/6.37	28	Enolase I-like, hypothetical protein LOC433182 [<i>Mus musculus</i>]
R23,26		24159081	133	28498/6.41	41	Chain A, crystal structure analysis of rat enoyl-coA hydratase in complex with hexadienoyl-coA

(continued on next page)

Table 3 (Continued)

Spot no.	Identified AA sequence (MS/MS)	MATCHED protein	NCBI acc no.	Score	Mr/pI	seq.cov
	K.FLSHWDHTR.I					
	K.AQFGQPEILLGTTIPGAGGTQR.L					
	K.SLAMEMVLTGDR.I					
	K.IFPVETLVEEAIQCAEK.I					
	K.LFYSTFATDDRR.E					
	R.EGMSAFVEKR.K					
R24	-.MAEYGEIIEGCRLPVLR.R Oxidation (M) R.RNQDNEDEWPLAEILSVK.D K.NGLPGRPGSPEREVPASAQASGK.T R.FNLPKER.E R.MTGSLSVDRSHDDIVTR.M K.TLYYDITDPFLFYVMTEYDCK.G	PREDICTED: HIV-1 Tat interactive protein, 60 kDa isoform 4 [Macaca mulatta]	109105458	75	50824/8.74	23
R27	M.PGGLLLGDEAPNFEANTTIGHIR.F R.FHDFLGDWSGILFSHPR.D R.DFTPYCTTELGR.A K.LAPEFAKR.N K.LIALSIDSVEDHFAWSK.D R.VVFIFGPKK.L K.LKLSILYPATTGR.N K.LSILYPATTGR.N R.NFDEILR.V R.VVDSLQLTASNVPVATPVDWK.K	Peroxiredoxin 6 [Rattus norvegicus]	167583348	188	24860/5.64	56
R29	R.YVQQNAKPGDPQSVLEAIDTYCTQK.E K.EWAMNVGDAK.G K.QIMDAVIR.E K.QIMDAVIR.EOxidation (M) R.EYPSLVLELGAYCYGSAYR.M R.YLPDITLLLEK.C R.KGTVLLADNVIVPGTPDFLAYVR.G K.GTVLLADNVIVPGTPDFLAYVR.G R.GSSSECTHYSSYLEYMK.V K.AIYQGPSSPKS.- R.VDYGGVTVDELGK.V	Chain, catechol O-methyltransferase	1633081	161	24960/5.11	57
R28		Phosphatidylethanolamine binding protein [Rattus norvegicus]	8393910	134	20902/5.48	62

K.LYTLVLTDPDAPSR.K
 K.FREWHHFLVNNMK.G
 K.FREWHHFLVNNMK.GOxidation (M)
 K.GNDISSGTVLSEYVGSPPK.D
 K.GNDISSGTVLSEYVGSPPKDTGLHR.Y
 R.YVWLVEEQEQLNCDPILSNK.S
 K.FKVESFR.K
 K.YHLGAPVAGTCFQAEWDDSVPK.L

Other ubiquitous protein

R3 K.HGDGVKDIAFEVEDCEHIVQK.A
 K.FAVLQTYGDTTHTLVEK.I
 R.FWSVDDTQVHTEYSSLR.S
 R.SIVVANYEESIK.M
 R.SIVVANYEESIKMPINEPAPGR.K
 K.MPINEPAPGR.K.K
 K.SIQEYVDYNGGAGVQHIALR.T
 R.GMEFLAVPSSYYR.L
 R.GMEFLAVPSSYYR.L Oxidation (M)
 R.HNHQGFAGNFNSLFK.A

202924
 43591/6.31
 129
 43591/6.31
 34

F alloantigen,
 4-hydroxyphenylpyruvic
 acid dioxygenase
 [*Rattus norvegicus*]

R5 R.GRFLHFHSVTFWVGNK.Q
 K.HGDGVKDIAFEVEDCEHIVQK.A
 K.FAVLQTYGDTTHTLVEK.I
 R.FWSVDDTQVHTEYSSLR.S
 R.SIVVANYEESIKMPINEPAPGR.K
 R.GMEFLAVPSSYYR.L
 R.GMEFLAVPSSYYR.L Oxidation (M)
 R.HNHQGFAGNFNSLFK.A

202924
 43591/6.31
 82
 43591/6.31
 32

F alloantigen,
 4-hydroxyphenylpyruvic
 acid dioxygenase
 [*Rattus norvegicus*]

Cytoskeleton

R18 .PRAVPSIVGR.S
 R.AVPSIVGR.S
 K.IWHHTFYNELR.V
 R.VAPEEHPVLLTEAPLNPK.A
 R.DLTDYLMK.I
 R.GYSFTTAER.E
 K.SYELPDGQVITIGNER.F
 K.DLYANTVLSGGTMYPGIADR.M
 K.IKIAPPER.K
 K.IIAPPERK.Y

49868
 39446/5.78
 174
 39446/5.78
 30

Put. beta-actin (aa 27-
 375) [*Mus musculus*]

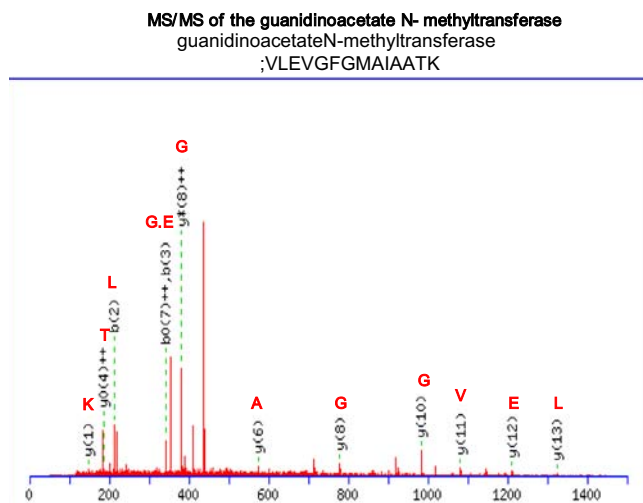


Fig. 6 MS/MS spectrum of the VLEVGFGMAIAATK digested peptide from guanidinoacetate N-methyltransferase. b-ions(b), double charged b-H₂O ion (b^{o++}), y-ions (y), double charged y-NH₃ (y^{o++}), and double charged y-H₂O (y^{o++}) ions of tryptic digestion of peptide VLEVGFGMAIAATK were identified. The ion identification is indicated in spectra panel (Table 8).

fatty acids, including acyl-CoA dehydrogenase and enoyl-CoA hydratase, and even the cholesterol synthesis regulatory enzyme β -hydroxy β -methyl glutaryl CoA reductase.

Camels can tolerate starvation while maintaining a constant nitrogen balance with urea nitrogen recycling [21]. Keeping available nitrogen is essential resource for synthesis of other bioactive nitrogenous molecules including creatine. Creatine phosphate is among the most important energy currency of the cell. This is the first report of enhanced levels of guanidinoacetate methyltransferase in a liver proteome. Guanidinoacetate methyltransferase, a key enzyme of creatine phosphate synthesis, has more protective role on Na⁺, K⁺-ATPase, and mitochondrial creatine kinase activities and an antioxidant role against lipid peroxidation and guanidinoacetate accumulation [22]. This suggests an additional homeostatic mechanism in camel hepatocytes.

Building new biopolymers is facilitated with guaranteed available energy accompanied by suitable anti-misfolding chaperones and adequate cytoskeleton proteins. Rapid intra- and/or intercellular communication are enforced by the presence of annexin cytoskeleton in camel liver proteome. Antioxidant glutathione peroxidase may afford an extra hepatocellular adaptive mechanism in camel against either heat-induced and/or acid-induced amorphous aggregation of proteins. Mitochondrial import stimulation factor is a known cytoplasmic chaperone specific for mitochondrial precursors [23]. It is related to 14-3-3 protein epsilon. This ubiquitous eukaryotic protein family exhibits a wide range of protein interaction-mediated regulatory and chaperone properties with phosphorylation-dependent affinity. Phosphorylated proteins have much higher affinity when compared with non-phosphorylated ones, explaining the role of 14-3-3 proteins in controlling protein kinases and other cellular events including autophagy and tumorigenesis through Beclin 1 phosphorylation [24,25]. Previous investigation has extended the role of 14-3-3 protein in the interaction with different Na⁺/Ca²⁺ exchangers. This maintains a low free Ca²⁺ concentration

within the vital cellular limit, by regulating their function, and, as a result, Ca²⁺ signaling in the cell [26].

Hump fat proteome: A dynamic rather than quiescent homeostatic domain

Adipocytes play a central role in energy balance by serving as major site of storage and energy expenditure [27]. The relatively high abundance of low molecular weight and low pI proteins in hump fat suggests an enhanced tolerance toward acidity and a prominent involvement in cellular events. Camel hump fat displayed more proteins than rat adipose tissue, suggesting a more metabolically active tissue. In addition to a well-developed cytoskeleton, containing actin and tubulin, the data confirm the presence and the high levels of vimentin. Moreover, vimentin's essential role in the signal transduction pathway from ss3AR to the activation ERK and its contribution to lipolysis [28] makes vimentin an early marker of adipogenesis. Vimentin regulates lipid droplet content during differentiation [29,30] and controls the key signaling components of lipid raft processing. [31]. Moreover, the higher level of glucagon in camel with consequent elevated basal blood glucose [2] is consistent with the proposed role of vimentin in GLUT-induced adipocyte glucose transport [32]. These data suggest a possible modulating role of adipocyte vimentin for the tolerance of high blood glucose levels in camel. Vimentin might operate as an inducer of a cellular trap for glucose in behalf of adipocyte energy storage. Furthermore, the dynamic nature of vimentin could offer the flexibility of fat cells. Since vimentin provides cells with resilience during mechanical stress *in vivo*, it may response for maintaining cell shape, integrity of its cytoplasm, and stabilizing cytoskeletal interactions. The observed high abundance of vimentin in camel adipocytes could promote the morphology of the hump of the well-nourished camel and can be considered as an adaptive correlate beneficial for living in arid conditions.

Cytochrome b5, a component of dromedary hump tissue, is a membrane bound hemoprotein, which functions as an electron carrier for several membrane bound oxygenases. Its presence in camel fat indicates a well-developed enzymatic system contributing to the detoxification of xenobiotics. Moreover, the conserved domains of cytochrome b5, with rabbit sharing a common sequence (40–89 amino acids residues), supports the extensive homology of this ortholog gene.

Galectin-1, β -galactoside-binding soluble 1 (L-14-I), is a component of dromedary adipocyte. Galectin-1 is widely expressed in epithelial and immune cells, contributing to the control of basic cellular processes, such as proliferation, apoptosis, and signal transduction, and immune modulation [33]. The present investigation suggests a similar role in camel adipocyte metabolism as described for other mammals [34]. The region of interest (residues 69–75) matches carbohydrate-recognition domain. Since the identity of galectin from different mammalian species is 80–90% [35], it is likely that galectin-1 also functions similarly.

Brain proteome

β -Synuclein has been shown to act as chaperonin inhibiting the fibrillation of α -synuclein [36]. The overexpression of β -synuclein in camel brain suggests an additional mechanism to prevent neurodegeneration in brain under intensive environmental stress.

Table 4 Identified camel hump fat proteins in NCBI database search GI; NCBI gene bank ID, Mw; molecular weight, pI; isoelectric point.

Spot no.	Identified AA sequence (MS/MS)	MATCHED protein	NCBI acc no.	Score	Mr/pI	Seq.cov
Hump fat						
<i>Cytoskeleton</i>						
C5	K.SYELPDGQVITIGNER.F K.DLYANTVLSGGTMYPGIADR.M K.QEYDESGPSVHR.K Proteins matching the same set of peptides:	Gamma non-muscle actin (<i>Oryctolagus cuniculus</i>)	1703	324	41729/5.30	13
C11	R.VAPEEHPVLLTEAPLNPK.A R.TTGIVMDSGDGVTHVPIYEGYALPHAIL Proteins matching the same set of peptides	Mostly gamma non-muscle actin and/or actin in many different species Putative beta-actin (amino acid 27–375) (<i>Mus musculus</i>)	49868 63007 71620 49868	324 324 324 123	39161 41809 41724 39161/5.78	13
C30	R.AILVDLEPGTMDSVR.S K.GHYTEGAELVDSVLDVR.K Proteins matching the same set of peptides	Actin beta rat Gamma actin (<i>Mus musculus</i>) Unnamed protein product (<i>Rattus norvegicus</i>);beta tubulin	309090 1335823 57429	123 123 84	41667 41740 49931/4.79	7
<i>Metabolic enzymes and enzyme like protein</i>						
C1	K.EVGVGFATR.K K.NTEISFKLGQEFDEVTDDR.K Proteins matching the same set of peptides	Beta tubulin (<i>Homo sapiens</i>) Beta 3 tubulin (<i>Gallus gallus</i>) Predicted similar to tubulin, beta 3 isoform 2 (<i>Canis familiaris</i>)	158743 1297274 73956775	84 84 84	49812 50485 50648	
C2	MS, 29 peptide Matched from 65	Adipocyte lipid-binding protein (<i>Oryctolagus cuniculus</i>)	4887137	290	12528/7.71	25
C3	MS, 12 peptide matched from 65	Adipose-type fatty acid binding protein (<i>Spermophilus tridecemlineatus</i>)	12802820	290	14756	
C4	MS, 11 peptide matched from 65	Predicted: similar to fatty acid binding protein, adipocyte Predicted: similar to centromere protein F mKIAA0421 protein (<i>Mus musculus</i>)	73997350 76638067 37359936	290 52 49	14687 353257/5.01 76263/7.96	
C6	MS, 12 peptide matched from 65	Predicted: similar to ATP-binding cassette subfamily A member 3, partial [<i>Danio rerio</i>]. Predicted: similar to type I hair keratin KA27 (<i>Bos Taurus</i>)	68424078 76649749	61 47	55936/6.36 52545/4.78	
C7	K.NTEISFKLGQEFDEVTDDR.K Proteins matching the same set of peptides	Adipocyte lipid-binding protein (<i>Oryctolagus cuniculus</i>) Predicted: similar to fatty acid binding protein, adipocyte	4887137 12802820	142 142	12528/7.71 14756	17
C8	MS, 14 peptide matched from 65	Predicted: similar to CG31643-PA isoform 1 (<i>Bos Taurus</i>)	73997350, 76677435	142 51	14687 96302/8.31	

(continued on next page)

Table 4 (Continued)

Hump fat		MATCHED protein	NCBI acc no.	Score	Mr/pI	Seq.cov
Spot no.	Identified AA sequence (MS/MS)					
C10	MS, 15 peptide matched from 65	Predicted: similar to protein transport protein Sec2	73952947	44	111485/6.87	
C12	MS, 12 peptide matched from 65	Predicted: similar to aldolase reductase	76662094	52	34311/5.34	
C13	K.DGGAWSGEQR.E K.LPDGYEFK.F	Galectin-1 (beta-galactoside-binding lectin 1-14-1) lactose binding lectin 1)	3122339	120	14694/5.37	13
C14	K.LISWYDNEFGYSNR.V Proteins matching the same set of peptides	glyceraldehydes-3-phosphate dehydrogenase (<i>Drosophila hydei</i>) Glyceraldehydes-3-phosphate dehydrogenase (<i>Canis familiaris</i>)	11178 50978862	118 118	35359/8.20 35838	4
C16	MS, 10 peptide matched from 65	Predicted: glyceraldehydes-3-phosphate dehydrogenase (<i>Pan troglodytes</i>)	55637711	118	36030	
C20	MS, 5 peptide matched from 65	Apoptosis inhibitor ch-1API (<i>Gallus gallus</i>)	11991646	46	36543/6.36	
C22	MS, 18 peptide matched from 65	Predicted: similar to mitochondrial ribosomal protein	68437845	51	7433/11.19	
C24	MS, 9 peptide matched from 65	Novel protein similar to vertebrate adenylate cyclase	56207901	54	86625/8.60	
C27	K.FLEHPGGEEVLR.E R.EQAGGDATENFEDVGHSTDR.E K.TFIIGELHPDDR.S Proteins matching the same peptides	Predicted: similar to ku70-binding protein 3 Cytochrome b5(sequence coverage 34%, sequence homology in the center of 134 amino acids polypeptide)	72014818 117811	50 156	22290/6.03 15340/5.16	34
C28	MS, 10 peptide matched from 65	Soluble cytochrome b5 (<i>Oryctolagus cuniculus</i>)	471150	156	11226	
C29	MS, 20 peptide matched from 65	Peditoxin, pedin = cytochrome b-like heme protein (<i>Toxopneustes pileolus</i> ; sea urchin) Predicted: similar to isocitrate dehydrogenase (NADP) F box and leucine rich repeat protein 10 isoform b	837345 74005287 54112380	156 49 46	9453 46777/6.13 144676/8.74	
<i>Chaperone like proteins</i>						
C15	R.VSLDVNHFAPPELTVK.T Proteins matching the same peptides	Heat shock protein 27 (<i>Rattus norvegicus</i>) HSP2DT (small heat shock protein (C-terminal) (Mice, peptide partial, 119 aa)) Heat shock protein 1 (<i>Mus musculus</i>) Vimentin (<i>Homo sapiens</i>)	204665 545503 7305173 37852	52 52 52 106	22879/6.12 12981 22887 53653/5.06	7
C17	R.EMEENFAVEAANYQDTIGR.L R.ISLPLPNFSSLNLR.E	Vimentin (<i>Homo sapiens</i>)	6563208 340234	49 99	54744/5.41 35032/4.70	19
C18	MS, 10 peptide matched from 65	Heat shock protein hsp70-related protein (<i>Homo sapiens</i>) Vimentin				
C23	R.EMEENFAVEAANYQDTIGR.L R.EYQDLLNVK.M R.ISLPLPNFSSLNLR.E R.DGQVINETSQHDDLE Proteins matching the same peptides	Vimentin (<i>Pan troglodytes</i>) Vimentin (<i>Homo sapiens</i>) Vimentin	56342340 62414289 340234	336 336 86	53615 53619 35032/4.70	19
C25	R.EMEENFAVEAANYQDTIGR.L R.EYQDLLNVK.M R.ISLPLPNFSSLNLR.E R.DGQVINETSQHDDLE Proteins matching the same peptides	Vimentin (<i>Pan troglodytes</i>) Vimentin (<i>Homo sapiens</i>)	56342340 62414289	314 314	53615 53619	

Other ubiquitous protein	Protein description	Accession	Count	Mass (kDa)
C19	K.LVNEVTEFAK.G K.YLYEIA.R	Albumin precursor (<i>Felis catus</i>)	110	68615/5.46
C9	K.LVNEVTEFAK.G K.LCTVASLR.D	Albumin precursor (<i>Felis catus</i>)	110	68615/5.46
C21	K.LVNEVTEFAK.K Proteins matching the same peptides	Human serum albumin in a complex with myristic acid and tri-iodobenzoic acid Serum albumin (<i>Homo sapiens</i>) Prealbumin (<i>Equus caballus</i>) Albumin precursor (<i>Felis catus</i>) Serum albumin precursor	99 99 65 95 64	65993 69321 68554/5.95 67837 66429
C26	K.LVNEVTEFAK.G K.YLYEIA.R	Albumin precursor (<i>Felis catus</i>)	85	68615/5.46

Phosphatidylethanolamine binding protein is a lipid-binding protein that enhances acetylcholine synthesis with additional inhibitory action on MEK- and ERK-signaling pathways. Phosphatidylethanolamine binding protein in camel brain shows high homology to the bovine protein. Furthermore, the larger amounts found in camel brain when compared to rat brain do not show the same proteome spot, suggesting enhanced ERK signaling in camel brain, warranting further study.

Camel proteome and heat shock proteins

Despite a preliminary investigation on a 73 kDa heat shock protein (hsp 73) in camel [37], there are no recent reports on hsp in camel. In the current study, proteins with extensive homology to the hsp 65, hsp 27, and chaperonin 10 were found in various camel organs. Heat shock proteins defense against dehydration or thermal stress in arid environments.

General outlook and implication of a well-developed cytoskeleton

The entire economy of the cell is a function of the structure of its transport facilities. Cytoskeletal proteins sculpt the structural architecture of cells and are classified into three groups: microfilaments represented in our data finding by actin filaments; intermediate filaments e.g. vimentin as that found in hump fat cells; and microtubules as different kind of β -tubulin. Different cytoskeletal protein monomers can build into a variety of structures based on associated proteins. Actin filaments are dynamic with their length controlled by polymerization driven through nucleotide hydrolysis. Additionally, actin filaments act with microtubules as railroads for motor proteins carrying transport vehicles, unfolded/misfolded proteins, and chromosomes important for cell-cell communication and survival [13]. Widely distributed adherence junctions are self-assembled cadherins interacting with β -catenin, which binds α -catenin and in turn interact with the actin cytoskeleton [38]. Their overexpression in the heart together with actin enhances intracellular communication. In non-muscle cells, the cytoskeletal isoform is found along with microfilament bundles and adherence junctions that bind actin to the membrane. The almost tenfold increase in α -actinin2 expression in camel heart and the presence of β -tubulin as a major energy deterrent cytoskeleton in the camel brain confers stress adaptation to the camel while guaranteeing more flexibility in ion channel modulation [13] to keep pace with abrupt ionic imbalances associated with dehydration–rehydration cycles.

Cytoskeleton-cellular signaling possible interplay

The DVL-binding protein DAPLE and the marked expression of actins suggest a possible interplay between cytoskeleton and fine tuning of intracellular signaling in camel hepatic cells. DAPLE binds to Dvl and functions as a negative regulator of the Wnt signaling pathway [39]. The Wnt pathway (known as the wingless pathway in *Drosophila*) has a role in organ development in a number of species [40] with the potential of carcinogenesis development on sudden activation [41]. The inductive properties of Wnt signaling are mediated by setting free actin-bound β -catenin. The accumulated β -catenin is then translocates to the nucleus where it binds to T-cell factors and activates transcription of a

Table 6 Identified proteins camel brain in NCBI database search G1; NCBI gene bank ID, Mw; molecular weight, pI; isoelectric point.

Spot no.	Identified AA sequence (MS/MS)	Matched protein	NCBI acc no.	Score	M _r /pI	Seq.cov
Brain						
B1	K.FSP L T S N L I N L L A E N G R . L Proteins matching the same peptides	H +-ATPase subunit, OSCP = oligomycin sensitivity conferring protein H +-ATPase subunit, OSCP = oligomycin sensitivity conferring protein [swine, heart, peptide mitochondrial Mitochondrial ATP synthase, O subunit [<i>Bos taurus</i>] Similar to oligomycin-sensitivity conferral protein [<i>Bos taurus</i>] ATP synthase, H + transporting, mitochondrial F1 complex, O subunit (oligomycin-sensitivity conferring protein) [<i>Bos taurus</i>]	913531 913531	51 51	20932/9.76 20932	8
B2	K.LY T L V L T D P D A P S R . K K.G N N I S S G T V L S D Y V G S G P P K . G Proteins matching the same peptides	Phosphatidylethanolamine binding protein 1 (PEBP-1) (HCNPpp) (Basic cytosolic 21 kDa protein) [contains: Hippocampal cholinergic neurostimulating peptide (HCNP)] Chain, phosphatidylethanolamine binding protein from calf brain Chain A, structure of the phosphatidylethanolamine binding protein from bovine brain Phosphatidylethanolamine binding protein [<i>Bos taurus</i>]	1352725	148	21087/6.9	18
B3	R.I M N T F S V V P S P K . V + Oxidation (M) R.A V L V D L E P G T M D S V R . S R.A V L V D L E P G T M D S V R . S + Oxidation (M) R.A V L V D L E P G T M D S V R . S + Oxidation (M) R.I N V Y Y N E A T G G N Y V P R . A R.I N V Y Y N E A T G G N Y V P R . A Proteins matching the same peptides	Tubulin 5-beta [<i>Homo sapiens</i>]	4389366 6729706 75812940	148 148 148	20828 20956 21106	9
B4	K.E G V V Q Q V A S V A E K . T K.E G V V Q Q V A S V A E K . T Proteins matching the same peptides	Tubulin, beta-4 [<i>Homo sapiens</i>] Tubulin, beta-4, isoform CRA_b [<i>Homo sapiens</i>] Beta-synuclein (phosphoneuroprotein 14) (PNP 14) (14 kDa brain-specific protein)	21361322 119589485	193 193	50010 54946	9
B5	K.A Q S E L L G A A D E A T R . A Proteins matching the same peptides	Beta-synuclein (phosphoneuroprotein 14) (PNP 14) Beta-synuclein [<i>Homo sapiens</i>] Chain H, bovine F1-ATPase inhibited by Decd (dicyclohexylcarbodiimide) ATP synthase, H + transporting, mitochondrial F1 complex, delta subunit precursor [<i>Bos taurus</i>]	464424 2501106 4507111 11514063 28603800	67 67 67 55 55	14268/4.4 14495 14279 15056/4.53 17601	9
B6	K.V L L P E Y G G T K . V K.V L Q A T V V A V G S G S K . G	Chaperonin 10 [<i>Homo sapiens</i>]	4008131	127	10576/9.44	24

Table 7 Identified proteins camel kidney in NCBI database search GI; NCBI gene bank ID, Mw; molecular weight, pI; isoelectric point.

Spot no.	Identified AA sequence (MS/MS)	MATCHED protein	NCBI acc no.	Score	Mr/pI	Seq. cov
K1	R.TDLALILSAGDN.- K.LAEYTDLMLK.L + Oxidation (M) R.LLPVQENFLLK.F	Calbindin	575508	145	18613/4.6	20
	Proteins matching the same peptides	Unnamed protein product [<i>Mus musculus</i>]	26347175	145	30247	
		Calbindin-d28 k	203237	143	30225	
		Calbindin-28 K [<i>Mus musculus</i>]	6753242	143	30203	
		Cerebellar Ca-binding protein, spot 35 protein [<i>Rattus norvegicus</i>]	14010887	143	30203	

Table 8 The ion identification as indicated in spectra panel.

Ion type	Neutral Mr
a	[N] + [M] – CHO
a*	a-NH ₃
a ^o	a-H ₂ O
b	[N] + [M] – H
b*	b-NH ₃
b ^o	b-H ₂ O
c	[N] + [M] + NH ₂
d	a – Partial side chain
v	y – Complete side chain
w	z – Partial side chain
x	[C] + [M] + CO – H
y	[C] + [M] + H
y*	y-NH ₃
y ^o	y-H ₂ O
z	[C] + [M] – NH ₂

number of genes. Overexpressed actin is in accord with the favored homeostasis.

Conclusions

The present investigation tried to shed light on camel proteome as innovative central point to study mammalian evolution. Much of the data obtained for camel cannot fit with proteomics data for other mammals. This mismatch is not an artifact but rather support the peculiarity of the camel and in particular its adaptive nature. This study also confirms the conserved nature of many camel proteins. Thus, the camel proteome corresponds to a remote reference useful in developing a perspective of proteomic evolution among different species.

Conflict of interest

The author has declared no conflict of interest.

Acknowledgement

The authors are grateful for Dr. Moustafa Radwan for helpful assistance of this work.

Appendix A. Supplementary material

Supplementary data associated with this article can be found, in the online version, at <http://dx.doi.org/10.1016/j.jare.2013.03.004>.

References

- [1] Ali AY. The Meaning of the Holy Qur'an; Amana Publications. ASIN: B004H0G2P6, 2004; Sura 88, verse17.
- [2] Abdel-Fattah M, Amer H, Ghoneim MA, Warda M, Megahed Y. Response of one-humped camel (*Camelus dromedarius*) to intravenous glucagon injection and to infusion of glucose and volatile fatty acids, and the kinetics of glucagon disappearance from the blood. Zentralbl Veterinarmed 1999;A(46):473–81.
- [3] Eitan A, Aloni B, Livne A. Unique properties of the camel erythrocyte membrane, II. Organization of membrane proteins. Biochem Biophys Acta 1976;426:647–58.
- [4] Warda M, Zeisig R. Phospholipid- and fatty acid-composition in the erythrocyte membrane of the one-humped camel [*Camelus dromedarius*] and its influence on vesicle properties prepared from these lipids. Dtsch Tierarztl Wochenschr 2000;107:368–73.
- [5] Davidson A, Jaime T, Vannithone S. The Oxford companion to food. 2nd ed. USA: Oxford University Press; 15 October 2006. p. 68, 129, 266, 762. ISBN:0192806815.
- [6] Hamers-Casterman C, Atarhouch T, Muyldermans S, Robinson G, Hamers C, Songa EB, et al. Naturally occurring antibodies devoid of light chains. Nature 1993;363:6428–46.
- [7] Kim N, Lee Y, Kim H, Joo H, Youm JB, Park WS, et al. Potential biomarkers for ischemic heart damage identified in mitochondrial proteins by comparative proteomics. Proteomics 2006;6:1237–49.
- [8] Gay S, Binz PA, Hochstrasser DF, Appel RD. Modeling peptide mass fingerprinting data using the atomic composition of peptides. Electrophoresis 1999;25:3527–34.
- [9] Zubarev R, Mann M. On the proper use of mass accuracy in proteomics. Mol Cell Proteomics 2007;6:377–81.
- [10] Schmidt-Nielsen K, Crawford EC, Hammel HT. Respiratory water loss in camel. Proc R Soc Lond (B Biol Sci) 1981;211:291–303.
- [11] Ryan SD, Ferrier A, Kothary RA. Novel role for the cytoskeletal linker protein dystonin in the maintenance of microtubule stability and the regulation of ER-Golgi transport. Bioarchitecture 2012;1:2–5.
- [12] Calaghan SC, Le Guennec JY, White E. Cytoskeletal modulation of electrical and mechanical activity in cardiac myocytes. Prog Biophys Mol Biol 2004;29–59.

- [13] Usui T. Actin- and microtubule-targeting bioprobes: their binding sites and inhibitory mechanisms bioscience. *Biotechnol Biochem* 2007;71(2):300–8.
- [14] Lu L, Timofeyev V, Li N, Rafizadeh S, Singapuri A, Harris TR, Chiamvimonvat N. Alpha-actinin2 cytoskeletal protein is required for the functional membrane localization of a Ca^{2+} -activated K^{+} channel (SK2 channel). *Proc Natl Acad Sci* 2009;106(43):18402–7.
- [15] Narayan P, Meehan S, Carver JA, Wilson MR, Dobson CM, Klenerman D. Amyloid- β oligomers are sequestered by both intracellular and extracellular chaperones. *Biochemistry* 2012;20(46):9270–6.
- [16] Boussette N, Chugh S, Fong V, Isserlin R, Kim KH, Volchuk A, et al. Constitutively active calcineurin induces cardiac endoplasmic reticulum stress and protects against apoptosis that is mediated by alpha-crystallin-B. *Proc Natl Acad Sci* 2010;107:18481–6.
- [17] Hoover HE, Thuerlauf DJ, Martindale JJ, Glembotski CC. Alpha B-crystallin gene induction and phosphorylation by MKK6-activated p38. A potential role for alpha B-crystallin as a target of the p38 branch of the cardiac stress response. *J Biol Chem* 2000;275:23825–33.
- [18] Smith JB, Sun Y, Smith DL, Green B. Identification of the posttranslational modifications of bovine lens alpha B-crystallins by mass spectrometry. *Protein Sci* 1992;1:601–8.
- [19] Voorter CE, de Haard-Hoekman WA, Roersma ES, Meyer HE, Bloemendal H, De Jong WW. The *in vivo* phosphorylation sites of bovine alpha B-crystallin. *FEBS Lett* 1989;259:50–2.
- [20] Ecroyd H, Meehan S, Horwitz J, Aquilina JA, Benesch JL, Robinson CV, et al. Mimicking phosphorylation of alpha B-crystallin affects its chaperone activity. *Biochem J* 2007;401:129–41.
- [21] Mousa HM, Ali KE, Hume ID. *Comp Biochem Physiol A* 1983;74:715–20.
- [22] Kolling J, Wyse AT. Creatine prevents the inhibition of energy metabolism and lipid.
- [23] Komiya T, Hachiya N, Sakaguchi M, Omura T, Mihara K. Recognition of mitochondria-targeting signals by a cytosolic import stimulation factor, MSF. *J Biol Chem* 1994;269:30893–7.
- [24] Wang RC, Wei Y, An Z, Zou Z, Xiao G, Bhagat G, et al. Akt-mediated regulation of autophagy and tumorigenesis through Beclin 1 phosphorylation. *Science* 2012;6(6109):956–9.
- [25] Mackintosh C. Dynamic interactions between 14-3-3 proteins and phosphoproteins regulate diverse cellular processes. *Biochem J* 2004;381:329–42.
- [26] Pulina MV, Rizzuto R, Brini M, Carafoli E. Inhibitory interaction of the plasma membrane $\text{Na}^{+}/\text{Ca}^{2+}$ exchangers with the 14-3-3 proteins. *J Biol Chem* 2006;281:19645–54.
- [27] Spiegelman BM, Flier JS. Obesity and the regulation of energy balance. *Cell* 2001;104:531–43.
- [28] Kumar N, Robidoux J, Daniel KW, Guzman G, Floering LM, Collins S. Requirement of vimentin filament assembly for beta 3-adrenergic receptor activation of ERK MAP kinase and lipolysis. *J Biol Chem* 2007;282:9244–50.
- [29] Brasaemle DL, Dolios G, Shapiro L, Wang R. Proteomic analysis of proteins associated with lipid droplets of basal and lipolytically stimulated 3T3-L1 adipocytes. *J Biol Chem* 2004;45:46835–42.
- [30] Al Battah F, De Kock J, Ramboer E, Heymans A, Vanhaecke T, Rogiers V, Snykers S. Evaluation of the multipotent character of human adipose tissue-derived stem cells isolated by Ficoll gradient centrifugation and red blood cell lysis treatment. *Toxicol In Vitro* 2011;25:1224–30.
- [31] Meckes Jr DG, Menaker NF, Raab-Traub N. Epstein-Barr virus LMP1 modulates lipid raft microdomains and the vimentin cytoskeleton for signal transduction and transformation. *J Virol* 2013;87:1301–11.
- [32] Guilherme A, Emoto M, Buxton JM, Bose S, Sabini R, Theurkauf WE, et al. Perinuclear localization and insulin responsiveness of GLUT4 requires cytoskeletal integrity in 3T3-L1 adipocytes. *J Biol Chem* 2000;275:38151–9.
- [33] Dettin L, Rubinstein N, Aoki A, Rabinovich GA, Maldonado CA. Regulated expression and ultrastructural localization of galectin-1, a proapoptotic beta-galactoside-binding lectin, during spermatogenesis in rat testis. *Biol Reprod* 2003;68:51–9.
- [34] Kiwaki K, Novak CM, Hsu DK, Liu FT, Levine JA. Galectin-3 stimulates preadipocyte proliferation and is up-regulated in growing adipose tissue. *Obesity* 2007;15:32–9.
- [35] Barondes SH, Cooper DN, Gitt MA, Galectins Leffler H. Structure and function of a large family of animal lectins. *J Biol Chem* 1994;269:20807–10.
- [36] Yamin G, Munishkina LA, Karymov MA, Lyubchenko YL, Uversky VN, Fink AL. Forcing nonamyloidogenic beta-synuclein to fibrillate. *Biochemistry* 2005;44:9096–107.
- [37] Ulmasov HA, Karaev KK, Lyashko VN, Evgen'ev MB. Heat-shock response in camel (*Camelus dromedarius*) blood cells and adaptation to hyperthermia. *Comp Biochem Physiol B* 1993;106:867–72.
- [38] Nelson WJ, Nusse R. Convergence of Wnt, beta-catenin, and cadherin pathways. *Science* 2004;303:1483–7.
- [39] Oshita A, Kishida S, Kobayashi H, Michiue T, Asahara T, Asashima M, et al. Identification and characterization of a novel Dvl-binding protein that suppresses Wnt signalling pathway. *Genes Cells* 2003;8:1005–17.
- [40] Shackel N. Zebrafish and the understanding of liver development: the emerging role of the Wnt pathway in liver biology. *Hepatology* 2007;45:540–1.
- [41] Giles RH, van Es JH, Clevers H. Caught up in a Wnt storm: Wnt signaling in cancer. *Biochem Biophys Acta Rev Cancer* 2003;1653:1–24.